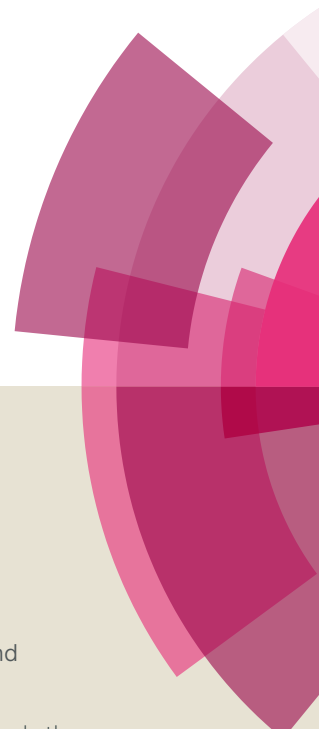


NJC

Accepted Manuscript



This article can be cited before page numbers have been issued, to do this please use: D. K. Pandey and P. Biswas, *New J. Chem.*, 2019, DOI: 10.1039/C9NJ01180C.



This is an Accepted Manuscript, which has been through the Royal Society of Chemistry peer review process and has been accepted for publication.

Accepted Manuscripts are published online shortly after acceptance, before technical editing, formatting and proof reading. Using this free service, authors can make their results available to the community, in citable form, before we publish the edited article. We will replace this Accepted Manuscript with the edited and formatted Advance Article as soon as it is available.

You can find more information about Accepted Manuscripts in the [author guidelines](#).

Please note that technical editing may introduce minor changes to the text and/or graphics, which may alter content. The journal's standard [Terms & Conditions](#) and the ethical guidelines, outlined in our [author and reviewer resource centre](#), still apply. In no event shall the Royal Society of Chemistry be held responsible for any errors or omissions in this Accepted Manuscript or any consequences arising from the use of any information it contains.

1
2
3 Production of propylene glycol (1, 2-propanediol) by the hydrogenolysis of glycerol in a fixed
4 bed downflow tubular reactor over highly effective Cu-Zn bifunctional catalyst: Effect of
5 acidic/basic support
6
7
8
9

10
11
12
13
14
15
16
17 Dinesh Kumar Pandey and Prakash Biswas*
18
19
20
21
22
23
24
25
26
27
28
29
30
31
32
33
34
35
36
37

38
39 Department of Chemical Engineering, Indian Institute of Technology Roorkee, Roorkee-247667,
40
41 Uttarakhand, India.
42
43
44
45
46
47
48
49
50
51
52
53
54
55
56
57
58
59
60

*Author to whom correspondence should be addressed: email: prakbfch@iitr.ac.in;
prakashbiswas@gmail.com,

Tel.: (+91)-1332-285184; Fax: +91-1332- 276535

Abstract

In this study, different acidic (V_2O_5 , ZrO_2 , TiO_2) and basic (CaO , MgO) oxides supported copper-zinc bimetallic catalyst were prepared by deposition-precipitation method and evaluated for vapor phase hydrogenolysis of glycerol to propylene glycol at 0.1 MPa and at 220°C. The catalysts were thoroughly characterized by different techniques such as BET, XRD, H_2 -TPR, NH_3 and CO_2 TPD, N_2O adsorptive decomposition, TEM, XPS, FE-SEM and TGA. Among all the supported catalysts, Cu-Zn/MgO catalyst was found to be the most selective to propylene glycol. High copper metal dispersion (~5%), surface area (~23 $m^2 \cdot g^{-1}$), highest basicity (0.25 $mmol CO_2 \cdot g \cdot cat^{-1}$) and the availability of partially reduced copper species (Cu_2O , CuO and Cu^0) were the primary reasons for higher propylene glycol selectivity. At optimum reaction condition i.e. at 220°C, 0.72MPa, and at the weight hourly space velocity (WHSV) of $0.073 h^{-1}$, ~98.5 % conversion of glycerol with ~89% selectivity to propylene glycol was obtained over Cu-Zn/MgO catalyst. The catalyst was found to be stable for longer period of time (84 h) without much deactivation and affecting the selectivity to propylene glycol.

Keywords: Glycerol hydrogenolysis, vapor phase, sectional packed downflow reactor, Cu-Zn/MgO catalyst, propylene glycol.

1. Introduction

Due to the scarcity of petroleum reserves and environmental issues, biodiesel has been regarded as one of the promising and acceptable alternatives to the conventional diesel. However, the major concern of the modern biodiesel industries is the value addition of the excess amounts (~10 wt.%) of low-grade glycerol obtained as a by-product [1,2]. The various routes for glycerol value addition have been reviewed and documented [3,4]. Among these, hydrogenolysis of glycerol to propylene glycol (1,2-propanediol) has received much attention in the last two decades because of very high demand of 1,2-propanediol (1,2-PDO) [5,6]. 1,2-PDO is a valuable chemical and widely used as a feedstock for the manufacture of unsaturated polyester resin, as a functional fluid, paints, cosmetics, starting materials in pharmaceuticals, printing etc. [5]. The production of 1,2-PDO from glycerol is not only a lucrative to biodiesel producer but also a green route as compared to the current commercial hydration of propylene oxide derived from petroleum resources [7,8].

Glycerol hydrogenolysis was attempted over various supported noble and non-noble metal catalysts, primarily in a liquid phase as summarised by various authors [5,6,9]. Therein noble metals were reported as less selective to 1,2-PDO due to their more affinity towards the C-C bond cleavage [10-13]. While among transition metals, copper-based catalysts were reported as more active and selective towards 1,2-PDO [14-18]. Hydrogenolysis in the liquid phase has many limitations including very high reaction pressure (0.1-8.0 MPa) [19, 20], structural damage to catalyst due to hydrolytic effect, difficulties in catalyst separation, catalyst leaching etc., which impedes its commercialization. Therefore, vapor phase hydrogenolysis of glycerol to 1,2-PDO in a continuous flow fixed bed reactor has gained significant interest now a day. As of now, very limited numbers of research publications are available on the production of 1, 2-PDO in vapor

1
2
3 phase hydrogenolysis of glycerol in a continuous flow reactor^[21-30]. Akiyama and his co-workers
4
5
6
7
8
9
10
11
12
13
14
15
16
17
18
19
20
21
22
23
24
25
26
27
28
29
30
31
32
33
34
35
36
37
38
39
40
41
42
43
44
45
46
47
48
49
50
51
52
53
54
55
56
57
58
59
60

phase hydrogenolysis of glycerol in a continuous flow reactor^[21-30]. Akiyama and his co-workers
[22, 31] reported 97% selectivity to 1, 2-PDO in presence of a commercial Cu/Al₂O₃ catalyst. The
experiments were conducted in a continuous reactor at various gradient temperature. 1, 2-PDO
yield was increased to ~2% in presence of Ag as a catalyst promoter^[24]. Ba doped Cu-Cr
catalyst rendered higher catalytic activity, however, 1,2-PDO selectivity was marginally
improved, the addition of Ba increased acidic sites on the catalyst surface^[27]. Huang et al.
2008^[32] developed Cu/ZnO/Al₂O₃ catalyst by precipitation method and reported 96.2 %
conversion of glycerol with 92.2 % selectivity to 1,2 PDO at 190°C, 0.64 MPa. It was suggested
that acid catalyzed dehydration of glycerol proceed over metal oxides (ZnO and Al₂O₃) and
hydrogenation of intermediate was facilitated by copper metal. SiO₂ supported Cu catalyst
prepared by ion-exchange technique showed 87% selectivity to 1,2-PDO at 255 °C and 1.5 MPa
pressure, the catalytic activity was found to be dependent to the metallic surface area^[23].

Most of these studies were carried out at higher H₂ to glycerol mole ratio and they were
devoid of stability analysis. Mitaa et al. (2015)^[33] reported 90% conversion of glycerol with
84% selectivity to 1,2-PDO in presence of Cu/SBA-15 catalyst. However, catalyst deactivation
was observed after 10 h of reaction. Ni-based catalysts were found to be poor selective to 1,2-
PDO, nickel metal promoted C-C bond breakage and lower alcohol, ethylene glycol, CH₄ and
CO were detected as a major product^[22,32,34]. Although Cu based catalyst shown excellent
activity, however, there are sufficient evidence for their poor stability. Since the long-time
stability is the prime requirement for a commercial catalyst, therefore, various techniques have
been employed to achieve higher stability of copper metal^[35]. Various studies were performed
over a series of Cu-ZnO based catalysts, where ZnO was reported as an anti-sintering agent^{[35,}
36]. For glycerol hydrogenolysis reaction particularly it was observed that ZnO promoted

hydrogenation capability of the catalyst [37] because ZnO adsorbed atomic hydrogen and acted as a hydrogen reservoir [56]. ZnO also promoted CuO reduction in Cu/ZnO catalyst [37]. Previous literature also suggested that incorporation of ZnO enhanced the acidity and basicity of the catalyst, which promoted the catalytic activity significantly [55]. It was proposed that glycerol hydrogenolysis proceed with glycerol dehydration to acetol via acid protonation of terminal hydroxide group, and further acetol hydrogenated to 1,2-PDO in presence of active metal sites of the catalyst [38,55,59]. While in basic condition glycerol first dehydrogenated to glyceraldehyde which subsequently dehydrated to 2-hydroxyacrolein. Further, the hydrogenation of 2-hydroxyacrolein produced 1,2-PDO [39,40]. Given the fact that glycerol dehydration facilitates on the acidic and basic sites, various mild and strong acidic oxide such as Al₂O₃, SiO₂, boehmite^[41], Cr₂O₃, ZnO, ZnO/ Al₂O₃ [31], HY, H-β, H-ZSM [42], Al₂O₃^[43], ZnO^[44] γ-Al₂O₃, SiO₂ [45] and basic oxide (MgO^[46], CeO₂^[21]), modified solid base(Mg-Al-O)^[47] supported catalysts were developed and their performance was discussed in terms of the nature of acidic/basic sites present of the catalysts. It was shown that in presence of bronsted acid sites glycerol converted to acrolin and lower alcohols whereas glycerol dehydration to acetol was favoured in presence of Lewis acid sites [41, 48- 50].

In contrast to that, few studies reported that the dehydration of glycerol to acetol was favoured in presence of active metal sites and independent to the acidic sites of the catalysts [20-22, 51]. Moreover, there is another opinion about the dehydration of glycerol to acetol. Cu species present as Cu⁺ protonated the glycerol to form acetol via dehydration and copper species at the state of Cu⁰, activated the hydrogen molecules [63]. Further, Vila et al [62] also explained that in reduced Cu/Al₂O₃ catalyst, the ratio of Cu⁰ / Cu⁺ was the governing factor for the conversion of glycerol to acetol and 1,2-PDO, respectively. In this context and aforesaid background,

development of a highly stable and bi-functional catalyst, capable of catalyzing glycerol dehydration and hydrogenation of dehydrated product to 1,2-PDO in vapour phase is highly desirable.

In this study, copper-zinc bimetallic catalysts supported on various acidic (TiO_2 , V_2O_5 , ZrO_2) and basic (MgO , CaO ,) oxide were synthesized by the deposition-precipitation method. The effect of support on the catalytic performance was evaluated and compared in a sectional packed, downflow tubular reactor. MgO supported copper-zinc catalysts was found to be most active, selective and stable. Almost complete conversion (~98.5%) with very high selectivity (~89%) to 1,2-PDO was obtained at very low reaction pressure (0.72 MPa). The presence of acidic sites (Cu^+ and Cu^{++}) distributed over the larger surface area of MgO supported catalyst and the availability of Cu^0 species, metal dispersion, and basicity were correlated to high selectivity to 1,2-PDO. The structural stability of the MgO supported catalyst was examined by the time-on-stream (TOS) study. The results demonstrated that the catalyst was very stable and selective to 1,2-PDO for 84 h.

2. Catalyst preparation and characterization

For catalyst synthesis, $\text{Cu}(\text{NO}_3)_2 \cdot 3\text{H}_2\text{O}$ (99.5%, Thomas Baker, India), $\text{Zn}(\text{NO}_3)_2 \cdot 6\text{H}_2\text{O}$ (98.5%, Thomas Baker, India) were used as metal precursors and MgO light (98 %, Thomas Baker, India), CaO (95 %, Thomas Baker, India), V_2O_5 (99 %, Thomas Baker, India), ZrO_2 (99%, Thomas Baker, India), TiO_2 (98 %, Thomas Baker, India) were used as catalyst support. NaHCO_3 (99.9 %, Thomas Baker, India) was used as the precipitating agent. The standard chemicals such as glycerol (99.9%, Thomas Backer Pvt. Ltd. India) 1, 2-PDO (99.99%, Merck Specialities, India), acetol (95%, Alfa Aesar), ethylene glycol (99%), 1-propanol (99%), 2-

1
2
3 propanol (99.5%), ethanol (99%) and methanol (99%) were used for calibration. Hydrogen
4 (99.99%) and nitrogen (99.99%) were procured from Sigma Gases New Delhi, India.
5
6
7

8
9 Cu-Zn bimetallic catalyst supported on MgO, CaO, V₂O₅, ZrO₂, and TiO₂ were
10 synthesized by deposition-precipitation technique [30]. For all the catalyst, copper to zinc metal
11 weight ratio was 7:3, and the total metal loading was kept constant at 50 wt.% in the catalyst.
12 During the synthesis, the required amount of metal precursors were dissolved in distilled water
13 and metal hydroxides were precipitated by the dropwise addition of 1 (M), NaHCO₃ solution
14 under continuous stirring till the solution pH reached to 8-9. Further, the required quantity of
15 support oxide was added and the slurry was stirred for 6 h followed by aging at ambient
16 condition for 12 h. After aging, the upper layer of liquid was spilled out and remaining thick
17 slurry was washed with distilled water and filtered in a vacuum filter. The filtered cake was dried
18 at 120°C for 12 h followed by calcination at 400°C for 4 h in air atmosphere. The synthesized
19 catalysts were designated as Cu-Zn/MgO, Cu-Zn/CaO, Cu-Zn/TiO₂, Cu-Zn/V₂O₅, and Cu-
20 Zn/ZrO₂.
21
22
23
24
25
26
27
28
29
30
31
32
33
34
35
36
37

38 The physicochemical properties of the catalysts were characterized by Nitrogen
39 adsorption-desorption technique, X-ray diffraction (XRD), temperature-programmed reduction
40 (TPR), temperature-programmed desorption (TPD), N₂O chemisorption and scanning
41 photoelectron spectroscopy (XPS). The morphology of the catalysts was obtained by field
42 emission scanning electron microscope (FE-SEM) and transmission electron microscope (TEM).
43 Nitrogen adsorption-desorption isotherms of all the catalysts were obtained at liquid nitrogen
44 temperature (-196°C) in a Micromeritics ASAP 2020 instrument. Prior to each analysis, catalyst
45 sample was vacuumed degassed at 200°C for 3 h. XRD pattern of fresh calcined and reduced
46 catalysts were recorded in Bruker AXS D8 Advance diffractometer with Ni filtered Cu-K α
47
48
49
50
51
52
53
54
55
56
57
58
59
60

1
2
3 monochromatized radiation source ($\lambda = 1.5418 \text{ \AA}$). Diffraction patterns were obtained at the 20
4 interval of 10-90° with the steps of 0.02°/s and a time constant of 3 s. The reduction behavior of
5 the catalysts was determined in a Micromeritics Pulse Chemisorb 2720 instrument following the
6 standard procedure mentioned in our previous study [17,30, 67]. The morphology of the catalysts
7 was obtained by FE-SEM (Carl Zeiss Ultra Plus microscope) and by TEM (Tecnai G² 20 S-Twin
8 TEM, FEI model), respectively. To record Fe- SEM images, catalyst sample was spread
9 homogeneously over the sample holder and coated with gold using sputter coater (Edwards
10 S150). TEM image was recorded by dispersing sample in pure ethanol and put it on the copper
11 grid coated with carbon. The oxidation state of the active metals in the catalyst was determined
12 by XPS in a PHI 5000 Versa Probe III, XPS spectrometer.
13
14
15
16
17
18
19
20
21
22
23
24
25
26
27
28
29
30
31
32
33
34
35
36
37
38
39
40
41
42
43
44
45
46
47
48
49
50
51
52
53
54
55
56
57
58
59
60

For XRD and XPS analysis of reduced catalyst, catalysts were reduced for 2 h under the
flow (20cc/min) of a gas mixture (10% Ar balance He) in a small quartz reactor at their
respective reduction temperature of catalysts obtained from TPR study. After reduction, catalyst
samples were flushed with He gas at same temperature for 1 h to remove trace impurity and
adsorbed H₂ present in the catalyst. After completion of reduction process, catalyst sample was
kept in vacuum desiccators for XRD and XPS analysis.

TPD experiments were performed in Micromeritics Chemisorb 2750 machine. Prior to
the analysis, catalyst was degassed at 200°C under the flow of He (20 cc/min) for 1 h and
subsequently reduced *in-situ* at their respective reduction temperature obtained from TPR
experiments for 2h under the flow of a gas mixture (10% H₂ and balance Argon). After
reduction, samples were flushed with He (20 cc/min) at the same temperature for 1 h in order to
remove trace of H₂ remained adsorbed over catalyst surface and cooled to room temperature.
After cooling, catalyst samples were saturated with the respective analysis gases for 1 h. The

analysis gas (10%NH₃ balance He for NH₃ TPD and pure CO₂ for CO₂ TPD) flow was maintained at 20 cc/min. After the saturation, to remove physically adsorbed ammonia or CO₂ He gas was flushed at a rate of 20cc/min for 1h. Thereafter, samples were heated from room temperature to 1000°C at a temperature ramp of 10°C/min and desorption of gas at different temperature was recorded with the help of a thermal conductivity detector.

The percentage copper metal dispersion and copper metallic surface area in the catalysts were measured by N₂O chemisorption technique in Micromeritics Chemisorb 2750 machine following the standard experimental procedure described in various literature [37, 72, 73].

3. Catalyst test

Hydrogenolysis of glycerol was conducted in a sectional packed, downflow tubular reactor (Chemito Technologies, India), the detail description of the experimental set-up is discussed elsewhere [29]. In a typical experiment, the catalyst was sectionally packed inside the reactor with the help of glass wool. Prior to each experiment, the catalyst was reduced *in-situ* at the reduction temperature of the individual catalyst obtained from TPR experiments for 3 h under the flow of hydrogen (50 cc. min⁻¹), followed by cooling the reactor at the desired reaction temperature. The reactor was pressurized with the help of a back pressure regulator connected at the reactor outlet. After achieving the desired reaction temperature and pressure inside the reactor, the feed was introduced into the reactor through an evaporator with the help of a liquid feed pump (Lab Alliance, USA, HPLC dosing type) and pre-mixed with the gas stream at the reactor inlet. The reaction was carried out at different conditions. Reaction pressure, temperature and weight-hourly-space-velocity (WHSV) was varied in the range of 0.1-0.8 MPa, 180-240°C, and 0.061-0.37 h⁻¹, respectively. The gas and liquid products were separated in a gas-liquid

separator connected at the outlet of the reactor. The products were analyzed in an online (GC 5765 Nucon, India) and offline (GC 6800, Newchrom Technologies, India) gas chromatography (GC), respectively. The online GC was equipped with a packed column (Porapak-Q) and a thermal conductivity detector (TCD). The offline GC was equipped with a flame ionization detector (FID) and a Chromosorb-101 packed column. Butanol was considered as an internal standard for product selectivity calculation. For, all the data reported in this study, the carbon balance was agreed 100 ± 5 %. The reported glycerol conversion, product selectivity, and product yields were calculated following the equations [(1)-(3)].

$$\text{Glycerol conversion (\%)} = [(\text{Initial moles of glycerol} - \text{Final moles of glycerol}) / \text{Initial moles of glycerol}] \times 100 \quad (1)$$

$$\text{Product selectivity (\%)} = [\text{Moles of carbon in the specific product} / \text{Total carbon in all the products}] \times 100 \quad (2)$$

$$\text{Yield (\%)} = [\text{Conversion (\%)} \times \text{selectivity (\%)}] / 100 \quad (3)$$

4. Results and discussion

4.1. Catalyst characterization

Nitrogen adsorption-desorption isotherms of copper-zinc bimetallic catalysts with different supports are shown in Figure 1. Typical type-IV isotherms were observed for irreversible capillary evaporation of condensed N_2 in the mesoporous structure of the catalysts [50]. A pronounced hysteresis loop at a relative pressure range of $0.5 < P/P_0 < 0.90$ were observed.

This result demonstrated a typical mesoporous nature of catalysts with hysteresis loop intermediate to type H₃ and H₄, indicated the presence of aggregate of plate-like particles with narrow slit-like pores within the catalysts^[51]. The obtained BET surface area (S_{BET}), total pore volume (V_p), Barrett–Jovner–Halenda (BJH) pore diameter (D_{BJH}) of catalysts are summarized in Table 1. The BET surface area was measured at the relative pressure (P/P_0) ranging from 0.05-0.3 and pore volume and pore size were calculated at P/P_0 of 0.987. The highest BET surface area of 55.5 m² g⁻¹ and pore volume of 0.17 cm³/g were obtained for MgO supported catalyst while the surface area (5.6 m². g⁻¹) and pore volume (0.05 cm³.g⁻¹) of CaO supported catalyst was lowest. The largest size pore (41.6 nm) obtained for CaO supported catalyst indicated the formation of large clusters of particles while pore size of other catalysts was in the range of 12.1-20.5 nm.

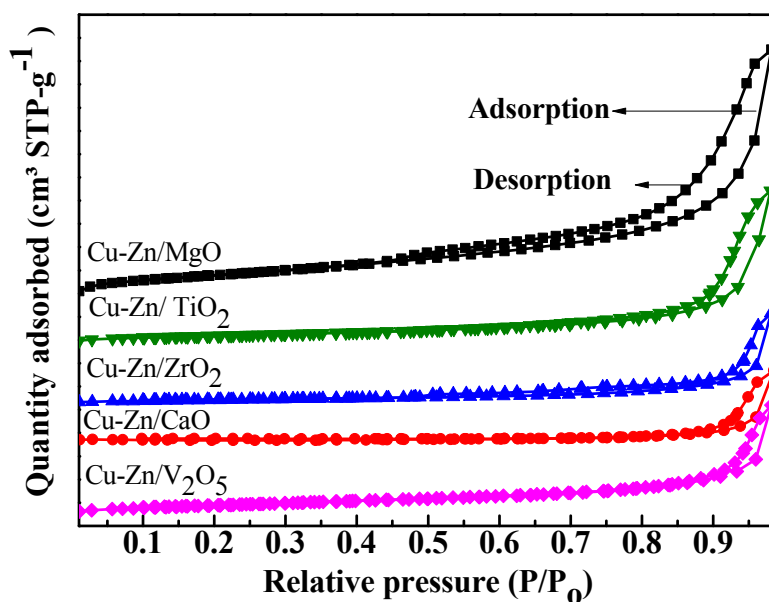


Figure 1. Nitrogen adsorption-desorption isotherms of catalysts. (a) Cu-Zn/MgO, (b) Cu-Zn/TiO₂, (c) Cu-Zn/ZrO₂, (d) Cu-Zn/CaO, (e) Cu-Zn/V₂O₅.

XRD

X-ray diffraction pattern of fresh calcined catalyst is displayed in Figure 2A. For all the catalysts, the peaks corresponding to CuO was detected at the 2θ value of 35.5° and 38.8° corresponding to (111) crystal plane [JCDPS-80-1916]. The characteristics peaks of ZnO were detected at the 2θ value of 31.7° , 34.6° , 56.5° , 62.8° , 67.8° corresponding to (100), (002), (110), (103) and (112) crystal planes, respectively [JCPDS-87-0075]. The diffraction peaks identified for various supports and their corresponding 2θ values are marked in Figure 2A.

The diffraction pattern of the reduced catalysts is shown in Figure 2B. The reduction temperature of individual catalyst was decided based on the TPR profile of the respective catalyst. The peaks corresponding to metallic copper were identified at the 2θ value of 43.1° corresponding to (111) crystal plane, at 50.2° correspond to (200) crystal plane and at 74.2° corresponding to (220) crystal planes, respectively [JCPDS-85-1326]. The diffraction peak corresponding to the (222) plane of cubic Cu_2O crystal was detected at the 2θ value of 36.4° [JCPDS-78-2076]. However, for (111) crystal plane of the cubic CuO phase was detected at the 2θ value of 35.4° and 38.2° , respectively [JCPDS-80-1268]. The peaks corresponding to metallic zinc was not detected in any catalysts and the peak corresponding to (100), (002), (110), (103), (112) crystal plane of ZnO was detected at the 2θ value of 31.2° , 34.4° , 56.5° , 62.8° , 67.8° , respectively [JCPDS-87-0075]. This results demonstrated that ZnO was not reduced to metallic zinc under the reduction condition used [54,74]. The characteristics diffraction peaks detected for MgO, TiO_2 , ZrO_2 and CaO are marked in Figure 2B. The diffraction peak corresponding to V_2O_5 was not detected in the reduced Cu-Zn/ V_2O_5 catalyst. For Cu-Zn/CaO catalyst, additional high-intensity peaks were detected at the 2θ value of 29.4° , 47.2° , 48.6° , respectively, corresponding to CaCO_3 [JCPDS01-086-017]. This results depicted that some of CaO might be converted to

1
2
3 CaCO₃ in presence of trace amount of bicarbonate present in the catalyst or the CaCO₃ could
4 have formed during calcination due to adsorption of ambient CO₂ [73]. The crystallite size of Cu,
5 CuO and ZnO was calculated by using the Scherrer equation and the values are displayed in
6 Table 1. The average crystallite size of Cu, CuO and ZnO was in the range of 26.4-32.5 nm,
7 17.1-35.5 nm and 24.5-55.5 nm respectively.
8
9
10
11
12
13
14
15
16
17
18
19
20
21
22
23
24
25
26
27
28
29
30
31
32
33
34
35
36
37
38
39
40
41
42
43
44
45
46
47
48
49
50
51
52
53
54
55
56
57
58
59
60

Table 1

Structural properties of catalysts

Catalyst	$S_{\text{BET}}^{\text{a}}$ ($\text{m}^2 \cdot \text{g}^{-1}$)	V_{p}^{a} ($\text{cm}^3 \cdot \text{g}^{-1}$)	$D_{\text{BJH}}^{\text{a}}$ (nm)	Copper metal dispersion (% D)*	Copper metal surface area* ($\text{m}^2 \cdot \text{g}^{-1}$)	Metal loading [#] (wt.%)		Crystallite size of calcined catalyst (nm)	Crystallite size of reduced catalyst (nm)	
						Cu	Zn		CuO	Cu
MgO	94.2	0.18	81.0	-	-	-	-	-	-	-
TiO ₂	23.0	0.034	16.0	-	-	-	-	-	-	-
ZrO ₂	14.0	0.012	6.9	-	-	-	-	-	-	-
CaO	6.8	0.02	14.0	-	-	-	-	-	-	-
V ₂ O ₅	27.6	0.04	13.8	-	-	-	-	-	-	-
Cu-Zn/MgO	55.5	0.17	12.6	4.88	23.1	41.8	12.8	25.8	27.0	50.0
Cu-Zn/TiO ₂	8.8	0.11	20.1	4.81	21.4	42.1	16.9	30.3	26.4	38.3
Cu-Zn/ZrO ₂	6.9	0.06	20.5	2.52	11.9	37.8	15.2	28.8	31.7	55.5
Cu-Zn/CaO	5.6	0.05	41.6	1.1	3.5	37.5	14.7	35.5	32.5	32.9
Cu-Zn/V ₂ O ₅	10.7	0.08	12.1	1.94	9.1	43.7	15.4	17.1	28.9	24.5

Note: ^aN₂ adsorption-desorption data, [#]SEM-EDX, *N₂O chemisorptions

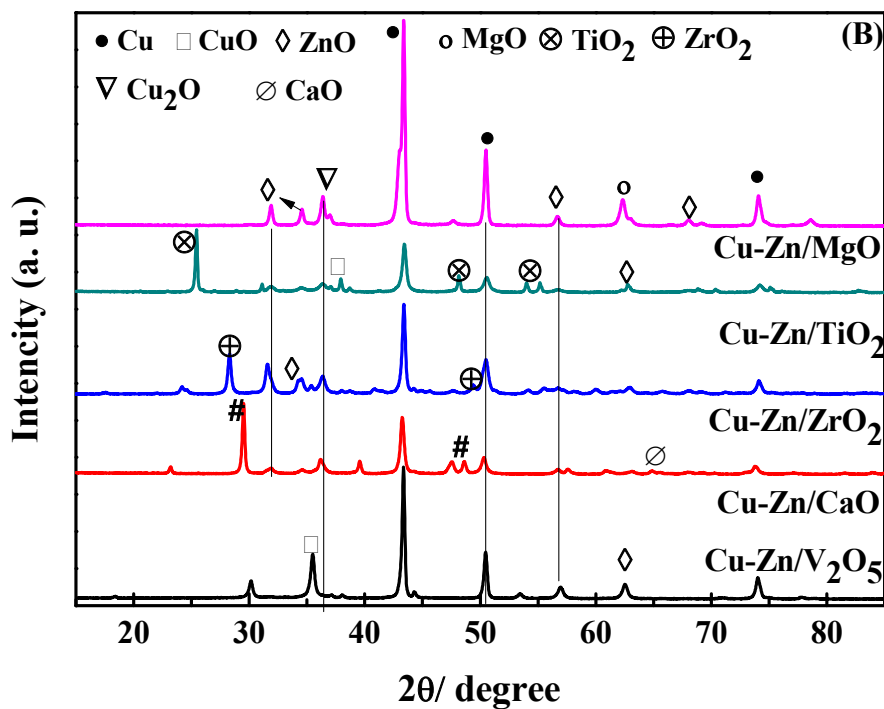
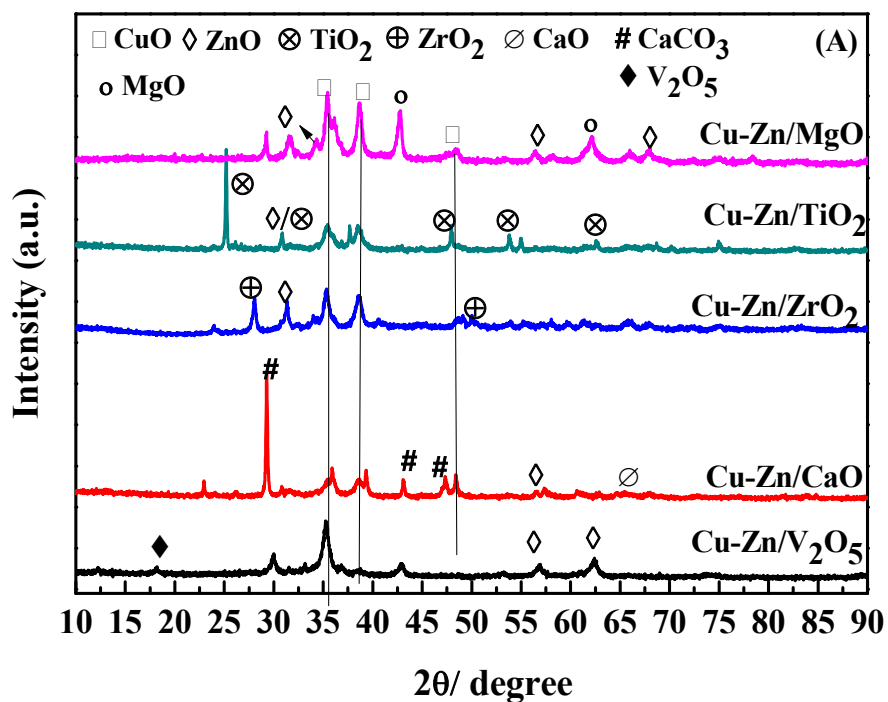


Figure 2. XRD patterns of (A) fresh calcined catalyst and (B) reduced catalysts

N₂O chemisorption

Copper metal dispersion and copper metal surface area in the catalysts were determined by N₂O chemisorption method and the obtained results are summarized in Table 1. The metal dispersion and metallic surface area of the catalysts followed the order as Cu-Zn/MgO > Cu-Zn/TiO₂ > Cu-Zn/ZrO₂ > Cu-Zn/V₂O₅ / Cu-Zn/CaO. The maximum metal dispersion (~4.9 %) and metallic surface area (23.1 m². g cat.⁻¹) were obtained for MgO supported catalyst. However, for CaO supported catalyst, the metal dispersion (~1.1 %) and metallic surface area (3.5 m². g⁻¹) was lowest. Large crystallite size and low surface area were obtained for Cu-Zn/ZrO₂ catalyst as compared to Cu-Zn/V₂O₅ catalyst. Still the metal dispersion was higher for Cu-Zn/ZrO₂ catalyst. This result indicated that metal support interaction also affected the distribution of active metals on the catalyst [74]. Metal dispersion and metallic surface area of different supported catalysts were dependent on the reduction–oxidation and reduction processes followed in N₂O chemisorptions technique. This reduction–oxidation and reduction behaviour varied in different catalysts due to their different metal-support interactions. Metal dispersion was lowest for Cu-Zn/CaO catalyst because of lowest surface area and due to higher degree of particle agglomeration as evident from FE-SEM images of calcined and reduced catalyst, respectively.

TPR

TPR patterns obtained for all the catalysts are shown in Figure 3. Since ZnO was not reducible in the temperature range studied, the reduction peaks obtained for all the catalysts were due to the combined reduction of CuO to Cu₂O and Cu₂O to Cu⁰, respectively [55, 56, 75]. For the Cu-Zn/MgO catalyst, the broad reduction peak was detected at (300-490°C), whereas the broad reduction peak was shifted to the slightly higher temperature (300-520 °C) for Cu-Zn/V₂O₅ catalyst. For Cu-Zn/TiO₂ and Cu-Zn/ZrO₂ catalyst, the reduction peaks were shifted to lower

temperature i.e. (250-370 °C) and (200-300 °C), respectively. For Cu-Zn/CaO catalyst the reduction peaks obtained at lower temperature was due to the reduction of CuO to Cu⁰ and higher temperature (>650°C) peak was may be due to the decomposition of CaCO₃. The lower side shifting of H₂ consumption peaks over TiO₂, ZrO₂ and CaO supported catalysts suggested that the reduction of Cu was facilitated over these supports [75]. The TPR patterns obtained clearly demonstrated the variation of metal support interactions in the different catalyst

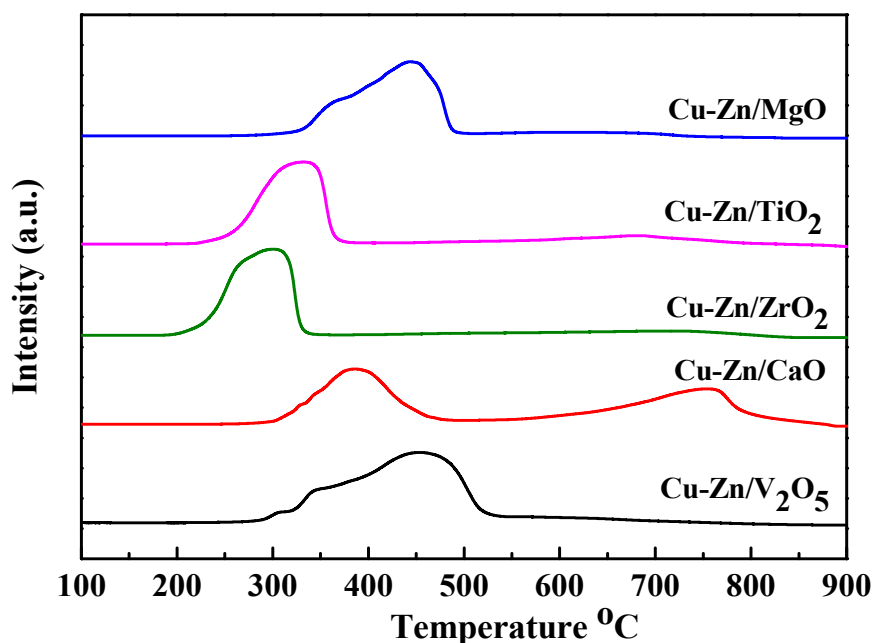


Figure 3 TPD profile of calcined catalysts.

TPD

The acidity and basicity of supports as well as catalysts was determined by NH₃-TPD and CO₂-TPD analysis, respectively. The NH₃ and CO₂ desorption pattern obtained for supports are shown in supplementary document [Figure 4(S)]. Total acidity and basicity of the support was calculated based on the total amount of NH₃ and CO₂ desorbed at different temperature region. Total acidity of the supports was in the range of 0.13-2.9 mmol NH₃ g cat.⁻¹. MgO was found to

1
2
3 be most acidic and ZrO_2 was the least acidic in nature. However, total basicity was in the range
4 of 0.03-1.17 mmol CO_2 . g cat.⁻¹. TiO_2 was the most basic and V_2O_5 was found to be the least
5 basic in nature.
6
7
8
9

10 The obtained desorption pattern of catalysts (Figure 4A) suggested desorption of
11 ammonia from weak (80-300°C), moderate (300-550°C) and strong (>550°C) acidic sites present
12 on the catalyst surface, respectively [17]. The total acidity of all the catalysts was varied in the
13 range of 0.057-1.12 mmol NH_3 . g cat.⁻¹ (Table 2). For Cu-Zn/MgO catalyst, total acidity was
14 found to be minimum (~ 0.057 mmol NH_3 . g cat.⁻¹). However, for the Cu-Zn/CaO catalyst, the
15 acidic sites were absent. The basicity of the catalyst was determined by CO_2 -TPD analysis.
16 Similar to the NH_3 -TPD pattern obtained, three different types i.e. weak, medium and strong
17 basic sites were detected (Figure 4 B). The obtained basicity on the catalyst surface was in the
18 range of 0.1-0.25 mmol CO_2 . g cat.⁻¹ (Table 2). Maximum basicity of ~0.25 mmol CO_2 . g cat.⁻¹
19 was obtained for Cu-Zn/MgO catalyst and it was lowest (~ 0.1 mmol CO_2 . g cat.⁻¹) for Cu-
20 Zn/ V_2O_5 catalyst. By comparison, it was observed that the acidity/basicity values of the support
21 material were affected significantly after the addition of metals as shown in Table 2.
22
23
24
25
26
27

28 To verify the NH_3/CO_2 desorption from the catalyst surface during TPD analysis
29 primarily at higher temperature (>500°C), a blank experiment was performed in absence of NH_3
30 and CO_2 . In the typical experiments, reduced catalyst was heated from room temperature to
31 1000°C at a temperature ramp of 10°C/min under the flow of helium (20 cc/min). Desorption was
32 monitored continuously with the help of a TCD. The results (Figure 3(S)) showed that, no
33 desorption peaks were detected for all the catalyst up to 1000 °C, except for CaO supported
34 catalyst. For CaO supported catalyst, a desorption peak was detected at 650-840°C due to the
35 decomposition of $CaCO_3$.
36
37
38
39
40
41
42
43
44
45
46
47
48
49
50
51
52
53
54
55
56
57
58
59
60

The NH_3 and CO_2 desorption pattern of Cu-Zn/CaO catalyst were plotted separately (Figure 4(C)). For this catalyst, a large desorption peak was detected at $>600^\circ\text{C}$, which indicated the decomposition of CaCO_3 at high temperature ($>600^\circ\text{C}$). The decomposition of CaCO_3 present in the Cu-Zn/CaO catalyst was also confirmed by the thermo-gravimetric analysis (TGA) (Figure 4(D)). Results demonstrated significant weight loss of the catalyst sample at $\geq 600^\circ\text{C}$, which is in agreement with the XRD, NH_3 -TPD and CO_2 -TPD results reported in Figure 4(C).

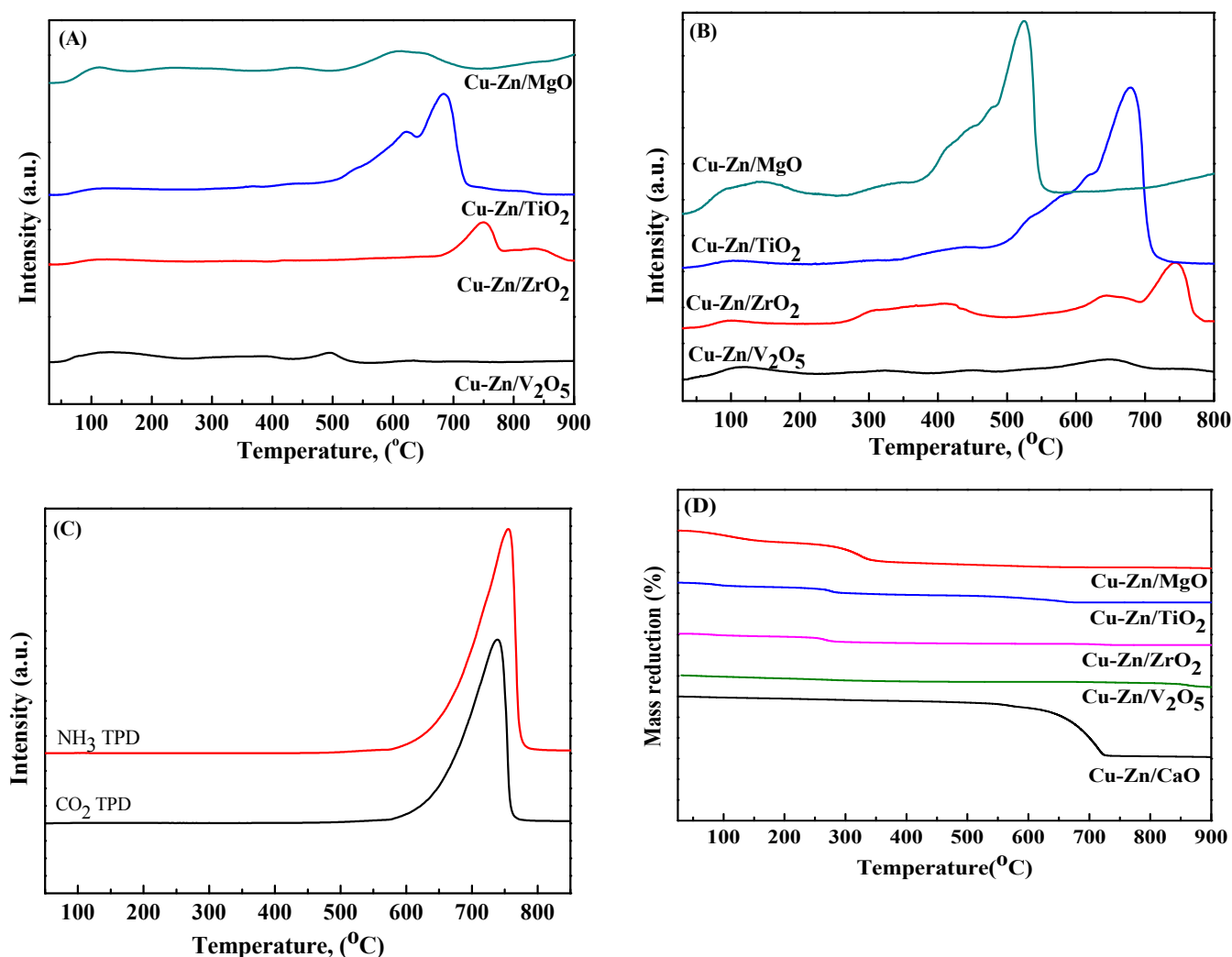


Figure 4. TPD profile of reduced catalysts (A) CO_2 -TPD and (B) NH_3 -TPD, (C) NH_3 and CO_2 TPD profile of Cu-Zn/CaO catalyst, (D) Thermogravimetric analysis of calcined catalysts.

FE-SEM

Morphology of supports and catalysts obtained from Field Emission Scanning Electron microscope (FE-SEM) are displayed in Figure 1(S) in the supplementary document. Rock like structure was detected for CaO and ZrO₂ support, while the morphology of MgO support was a layered flakes type. The morphology of TiO₂ has appeared as the mixture of quasi cylinders and spheres. The V₂O₅ support showed a combination of slits of different size. The morphology of all supported calcined catalysts exhibited the combination of rods and spherical shaped particles. However, after reduction, particles morphology was transformed into quasi-spherical structure. The SEM images obtained for different catalysts demonstrated the significant variation of catalyst morphology with the variation of supports, after calcination and reduction. The metal weight percentage obtained from SEM-EDX analysis is shown in Table 1. Theoretical and experimental values of metal percentage in the catalyst were in good agreement.

XPS

The existence of Cu⁰, Cu⁺, Cu⁺⁺ and ZnO species over the surface of reduced Cu-Zn/MgO catalyst was recorded in X-ray photoelectron spectrometer (XPS) and the XPS profile of Cu₂p_{3/2} and Zn₂p_{3/2} are displayed in Figure 2(S) (A) and (B), respectively. The single intense and wide spectrum at the binding energy in the range of 930eV-935eV was the indicator of the presence of Cu₂p_{3/2} species. The peaks referring to Cu⁰, Cu⁺ and Cu⁺⁺ at the binding energy range of 933-934eV were also reported earlier^[57, 58].

4.2. Catalytic activity

Catalytic activity was evaluated in a sectional packed bed, downflow tubular reactor. Initial catalyst screening was performed at 220°C, 0.1 MPa and at the WSHV of 0.18 h⁻¹. After starting the feed, the reaction was continued for 6 h to achieve a steady state. Further, the reaction data were collected after a regular time interval of 2 h. It was observed that glycerol conversion was increased up to 12 h and then it was almost unchanged for all the catalyst. Therefore, all the data reported in this study were collected after a reaction time of 12 h.

Initially, the activity of different support materials was evaluated at 220°C, 0.1 MPa and at the WSHV of 0.18 h⁻¹ and compared with the performances of supported catalysts. The results obtained are summarized in Table 2. As shown in Table 2, the activity of the supports was very poor. The highest glycerol conversion of 16.1% was obtained over CaO followed by TiO₂ (13.4%). The conversion obtained over other supports was < 7%. In presence of all the supports, acetol was detected as the main reaction product with the selectivity range of 45-55.2%, followed by 1-propanol (24.7-39.1 %), 2-propanol (7.2-11.1 %) and methanol (3.4-13.9%), respectively. 1,2-PDO was detected only in presence of ZrO₂ support with ~9% selectivity. This results demonstrated that, the role of the supports for selective hydrogenolysis of glycerol to 1,2-PDO was not very insignificant.

In presence of supported catalyst, the glycerol conversion and 1,2-PDO selectivity was increased significantly as shown in Table 2. The catalytic activity followed the order as Cu-Zn/CaO \approx Cu-Zn/MgO > Cu-Zn/V₂O₅ > Cu-Zn/ZrO₂ > Cu-Zn/TiO₂. Maximum glycerol conversion of 40-41% was obtained in presence of Cu-Zn/CaO and Cu-Zn/MgO catalyst, respectively. In presence of the supported catalyst, the primary reaction product was acetol. Cu-Zn/V₂O₅ catalyst showed the highest acetol selectivity of 89.5 % followed by Cu-Zn/CaO

(89.2%), Cu-Zn/TiO₂ (84.2%), Cu-Zn/ZrO₂ (83.0%) and Cu-Zn/MgO (76.6%), respectively. The obtained 1,2-PDO selectivity over various catalysts followed the order as Cu-Zn/V₂O₅ < Cu-Zn/CaO < Cu-Zn/TiO₂ < Cu-Zn/ZrO₂ < Cu-Zn/MgO. Maximum 1,2 PDO selectivity of 20.2 % was obtained over Cu-Zn/MgO catalyst. Results reported in Table 2 suggested that all catalysts were highly selective to acetol at atmospheric pressure because of low hydrogenation rate at ambient pressure due to the poor hydrogen adsorption [21, 32]. Trace amounts of other products including 1-propanol (1.1-2.1%), 2- propanol (0.7-1.8 %), and methanol (0.2-1.1 %) were also detected.

Gas phase dehydration of glycerol followed two different routes based on the nature of the acidic and basic sites present in the catalyst surface. Over the strong/bronsted acid sites, glycerol dehydrated to acrolein while moderately acidic centres/lewis acidic sites catalysed glycerol to acetol [41, 48- 50]. It has been reported that over Cu/Cr₂O₃ catalyst, at N₂ ambience, acetol was the primary product in the gas phase dehydration of glycerol at atmospheric pressure and at 230°C. At this condition, further hydrogenation of acetol to 1,2-PDO was insignificant [76]. However, in presence of bronsted acid sites incorporated by solid acids (niobium and tungsten oxide) on the Al₂O₃, SiO₂, and TiO₂ supports, glycerol was mainly dehydrated to acrolein at 305°C and at inert atmosphere [49]. Cu/ HZSM-5, Cu/ Hb catalysts were reported as less selective to 1,2-PDO as compared to Cu/Al₂O₃ catalyst due to their higher acidity. This results indicated that support had strong effect on the performance of the supported Cu base catalysts [42]. Sato et al. [21] investigated the catalytic performance of various acidic (Al₂O₃, SiO₂, ZrO₂, Fe₂O₃) and basic (MgO, CeO, ZnO) supported Cu catalysts for gas phase dehydration of glycerol at 250 °C and at N₂ atmosphere. Catalyst over acid oxide supports were shown as more selective to acetol as compared to basic oxide supported catalysts. From previous literature

1
2
3 discussion, major conclusion can be drawn that under strong acidic catalyst, glycerol was mainly
4 transformed to acrolein and dehydration of glycerol to acetol favored over moderately acidic
5 catalyst.
6
7
8
9

10
11 In this study, higher glycerol conversion over CaO and TiO₂ support and higher acetol
12 selectivity over all the support was possible due to combine effect of acid and basic nature of an
13 individual support. However, 1-propanol (1-PO) and 2-propanol (2-PO) were formed either
14 directly from glycerol or due to hydrogenolysis of 1,2-PDO in presence of bi-functional metal/acid-
15 base catalyst [77]. In contrast to that, X. Lin et al. [78] reported 69% selectivity to 1-propanol over
16 sequential two-layer H-β-Ni/Al₂O₃ catalysts at 220 °C, 2MPa H₂ pressure, due to hydrogenation
17 of acrolein. Manifold increased in glycerol conversion after the addition of Cu-Zn over the
18 supports suggested that metal species also participated in the process of dehydration as suggested
19 by various previous reports [20-22, 51].
20

21 The product distribution obtained clearly suggested that glycerol hydrogenolysis reaction
22 over Cu-Zn bimetallic catalyst in vapor phase followed the two simultaneous steps, initially,
23 acid/base sites of the catalysts catalyzed glycerol dehydration to acetol followed by metal
24 catalysis hydrogenation of acetol to 1,2-PDO [38, 59-61]. Higher selectivity to acetol suggested that,
25 at atmospheric pressure, dehydration of glycerol was favored. Results also demonstrated that the
26 activity trend obtained over various catalysts were not followed any regular trend with their
27 physicochemical properties i.e. acidity, basicity, BET surface area, metal dispersion (% D),
28 crystallite size obtained for all the catalysts. Although the percentage dispersion and metallic
29 surface area of MgO and TiO₂ supported catalysts were very close, still higher 1,2-PDO
30 selectivity over MgO supported catalyst indicated the intrinsic characteristic of this support for
31 this reaction.
32
33
34
35
36
37
38
39
40
41
42
43
44
45
46
47
48
49
50
51
52
53
54
55
56
57
58
59
60

Table 2

Acidity, basicity and catalytic performance

Catalyst	Conversion (%)	Selectivity (%)						Total Acidity (mmol NH ₃ . g cat. ⁻¹)	Total Basicity (mmol CO ₂ . g cat. ⁻¹)
		1,2-PDO	Acetol	1-PO	2-PO	Methanol	EG		
MgO	6.6	-	55.2	24.7	9.0	10.5	-	2.9	0.932
TiO ₂	13.4	-	51.6	38.2	10.2	-	-	2.07	1.17
ZrO ₂	3.6	8.95	48.2	27.5	7.2	7.4	-	0.13	0.056
CaO	16.1	-	52.4	26.1	7.5	13.9	-	-	-
V ₂ O ₅	5.8	-	45.0	39.1	11.1	3.4	-	1.61	0.029
Cu-Zn/MgO	40.3	20.7	76.6	1.2	0.7	1.1	0.5	0.057	0.25
Cu-Zn/TiO ₂	27.3	11.8	84.2	1.2	1.8	0.82	--	1.1	0.24
Cu-Zn/ZrO ₂	32.2	14.3	83.0	1.4	0.79	0.46	--	0.49	0.11
Cu-Zn/CaO	40.9	7.7	89.1	1.07	1.19	0.69	0.19	-	-
Cu-Zn/V ₂ O ₅	37.1	6.9	89.3	2.13	0.73	0.18	0.67	0.2	0.1

Reaction condition: 10 wt% aqueous glycerol solution, 220°C, 0.1 MPa, 1.0 g catalyst, H₂/glycerol mole ratio = 66.8, WHSV = 0.18 h⁻¹.

1
2
3 The basicity, copper metal dispersion (~5%) and the active metal surface area (~23 m². g⁻¹) was
4 highest for Cu-Zn/MgO catalyst. The uniform distribution of metal particles and the presence of
5 partially reduced Cu species (Cu₂O, CuO and Cu⁰) as evidenced from TEM and XRD results
6 were the governing factor for higher selectivity to 1,2-PDO in presence of Cu-Zn/MgO catalyst
7 [52]. The presence of Cu⁺ favored the dehydration of glycerol, while Cu⁰ activated the hydrogen
8 molecule for hydrogenation of intermediate acetol [63]. Since Cu-Zn/MgO catalyst was most
9 selective to 1,2-PDO, therefore, this catalyst was chosen further for detail reaction process
10 parameter study to increase the 1,2-PDO selectivity and yield. The time-on-stream stability of
11 Cu-Zn/MgO catalyst was also investigated.
12
13
14
15
16
17
18
19
20
21
22
23
24
25
26
27
28
29
30
31
32
33
34
35
36
37
38
39
40
41
42
43
44
45
46
47
48
49
50
51
52
53
54
55
56
57
58
59
60

4.3. Reaction parameter study

4.3.1. Effect of temperature

Effect of reaction temperature on glycerol conversion and product selectivity obtained over Cu-Zn/MgO catalyst at atmospheric pressure (0.1 MPa) is shown in Figure 5 (A). As expected, glycerol conversion was increased from 56.7% at 190°C to 92.3% at 260°C. At lower temperature (<200°C), acetol was obtained as the primary reaction product with very high selectivity (87.9 %) and the total selectivity to 1,2-PDO and other products was very low (~12.1 %). Acetol was formed as a primary product due to the dehydration of glycerol, whereas 1,2-PDO was obtained by the hydrogenation of acetol [63]. Further, with increasing the reaction temperature, it was observed that the selectivity to acetol was decreased with simultaneous increasing the selectivity to 1,2-PDO up to a reaction temperature of 240°C. Acetol selectivity was decreased from ~87.9 % to 67.9 % and the selectivity to 1,2-PDO was increased from 8.4% to 28.8% with increasing the reaction temperature from 190°C to 240°C. Moreover, within this

1
2
3 temperature range, the selectivity to other products was almost constant (~3.5%). This selectivity
4
5 trend suggested that, at the higher reaction temperature (>200°C), acetol was converted
6
7 selectively to 1,2-PDO by the hydrogenation process in presence of the active metal surface of
8
9 the catalyst [65]. At very high temperature (>240°C), the selectivity to 1,2-PDO was decreased
10
11 significantly with simultaneous increasing the selectivity to the other degradation products,
12
13 which indicated that very high temperature (>240 °C) facilitated 1,2-PDO degradation reaction
14
15 and produced the other products i.e. ethylene glycol, methanol, and ethanol, 1-PO and 2-PO,
16
17 respectively [65]. The effect of temperature variation at atmospheric pressure suggested that lower
18
19 reaction temperature (<240°C) was beneficial for higher selectivity to 1,2-PDO and the preferred
20
21 reaction temperature was ~ 220°C for higher selectivity to 1,2-PDO.
22
23
24
25
26
27
28
29
30
31
32
33
34
35
36
37
38
39
40
41
42
43
44
45
46
47
48
49
50
51
52
53
54
55
56
57
58
59
60

4.3.2. Effect of pressure

Influence of reactor pressure was investigated in the pressure range of 0.1 MPa to 0.8 MPa at 220°C, H₂/glycerol mole ratio of 66.8 and WHSV of 0.12 h⁻¹. As shown in Figure 5 (B), glycerol conversion was found to increase with pressure and nearly 98.3% conversion of glycerol was achieved at 0.72 MPa pressure. This is very interesting to note that, the selectivity to acetol was decreased drastically (~60%) with a sharp increase in selectivity to 1,2- PDO (~57.5 %) with increasing reaction pressure from ~0.12 to ~ 0.72 MPa at the constant reaction temperature of 220°C. Moreover, the variation in the selectivity to other products were very marginal (~2-3 %). This results demonstrated that, at lower pressure (~0.1 MPa), conversion of glycerol to acetol via dehydration reaction was highly favorable. However, with increasing reaction pressure from ambient to 0.72 MPa, acetol was converted to 1, 2- PDO by the hydrogenation reaction in presence of more hydrogen atom. At higher pressure, the higher concentration of active

hydrogen species on the metal site increased the rate of acetol hydrogenation to 1,2-PDO [32]. At very high pressure (i.e. > 0.72 MPa), 1, 2-PDO selectivity was started to decline due to over hydrogenolysis of 1, 2-PDO to lower alcohol [30]. The maximum 1,2-PDO selectivity 82.9 % was achieved at 0.072 MPa pressure.

4.3.3. Effect of catalyst amount

Reactions were conducted at 220°C and at 0.1 MPa pressure and the catalyst weight was varied from 0.5 g to 3.0 g. In each experiment, the catalyst was divided into two equal parts and placed sequentially over a glass wool bed inside the reactor. As shown in Figure 5(C), the glycerol conversion was increased sharply from 14.3% to 91.3% with increasing the catalyst amount up to 2 g and further it was gradually reached to 97.5 % in presence of 3 g of catalyst. The selectivity to acetol, 1,2-PDO and other products was also showed a similar trend as obtained with the variation of pressure. Selectivity to acetol gradually dropped from 88.1% to 53.6% against the slow rise of 1, 2-PDO selectivity from 10.7% to 39.1%. Increasing glycerol conversion and 1, 2- PDO selectivity were attributed to the accessibility of reactant to a higher number of active catalyst sites at higher catalyst loading as expected [67, 56]. Interestingly, no significant rise in other product selectivity was observed. Further increasing the catalyst weight (>3 g), increased the pressure drop inside the reactor, the maximum 1,2-PDO selectivity of 39.1 % was obtained in presence of 3 g catalyst.

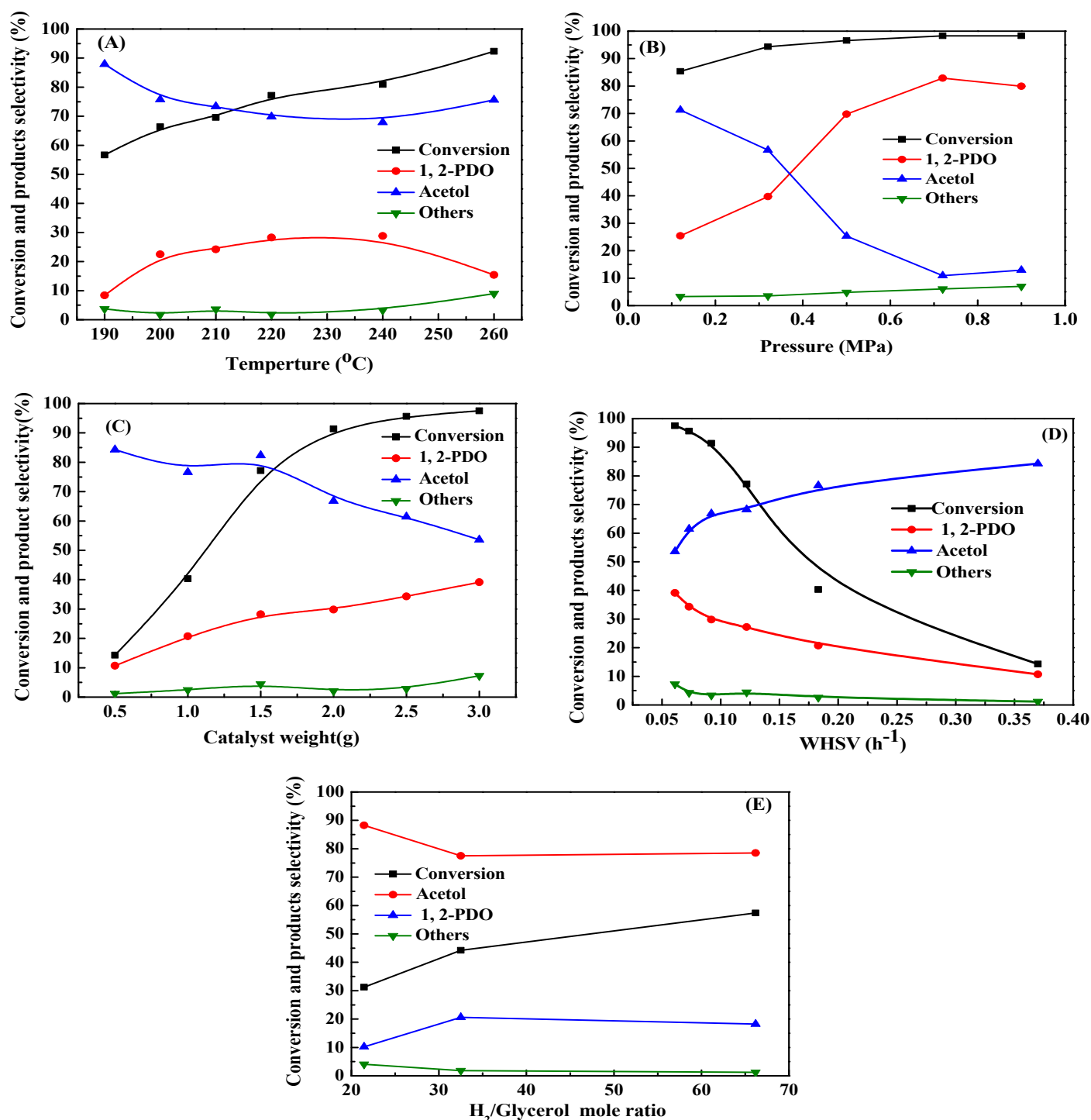


Figure 5. Variation of glycerol conversion and product selectivity over Cu-Zn/MgO catalyst.

(A) Effect of temperature (at 0.1 MPa, 1.5 g catalyst, WHSV 0.122 h⁻¹, H₂/glycerol mole ratio = 66.8). (B) Effect of pressure (at 220°C, 1.5 g catalyst, WHSV = 0.122 h⁻¹, H₂/glycerol mole

ratio= 66.8). (C) Effect of catalyst weight (at 220°C, 0.1 MPa, H₂/glycerol mole ratio = 66.8).

(D) Effect of weight hourly space velocity (at 220°C, 0.1 MPa, H₂/glycerol mole ratio = 66.8).

(E) Effect of Hydrogen to glycerol ratio (at 220°C, 0.1 MPa, catalyst weight 1 g).

*Others Methanol, 1-PO, 2-PO

4.3.4. Effect of weight hourly space velocity (WHSV)

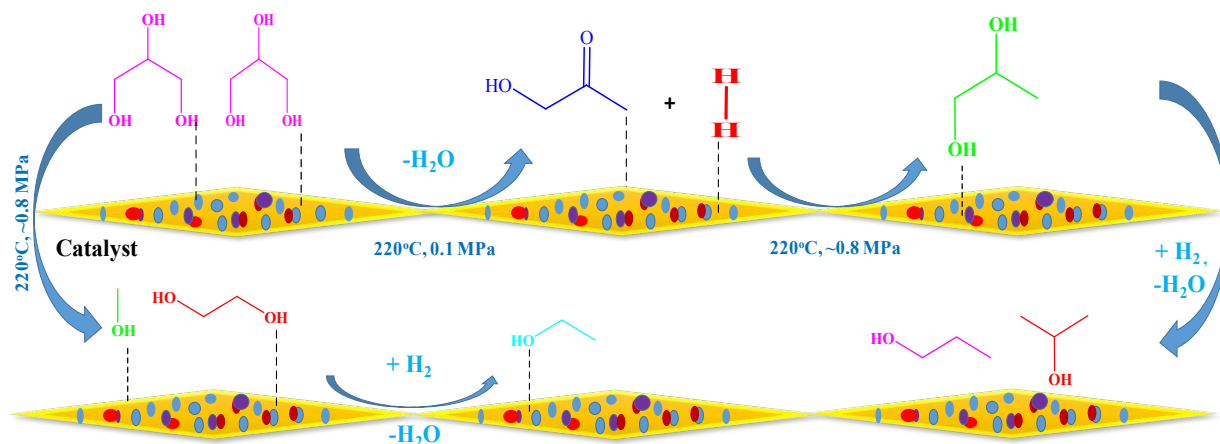
Variation of glycerol conversion and products selectivity in terms of WHSV (0.06-0.37 h⁻¹) are presented in Figure 5 (D). At the WHSV of 0.06 h⁻¹, the glycerol conversion was almost 100 % and a drastic drop in glycerol conversion and 1,2-PDO selectivity were observed with increasing the WHSV with simultaneous increasing the selectivity to acetol. The selectivity to other products was also decreased with WHSV. Poor access of reactants to active sites at higher WHSV may likely be the possible reason for diminishing the glycerol conversion and 1,2-PDO selectivity [67]. The maximum 1,2-PDO selectivity to 39.1% was obtained at the WHSV of 0.06 h⁻¹.

4.3.5. Effect of hydrogen to glycerol mole ratio

The variation in glycerol conversion and product selectivity obtained with the variation in H₂ to glycerol mole ratio is displayed in Figure 5 (E). The hydrogen to glycerol mole ratio was varied by varying the glycerol concentration in the feed. The results indicated that higher H₂/glycerol ratio favored high glycerol conversion and high selectivity to 1,2-PDO. However, at lower H₂/glycerol mole ratio, the glycerol conversion was decreased. This results demonstrated that lower glycerol concentration favored glycerol conversion and 1,2-PDO selectivity. Possibly higher glycerol concentration produced adsorption hindrance for hydrogen over the limited

1
2
3 catalyst surface and consequently diminished the acetol hydrogenation rate. It may be argued that
4
5 at higher glycerol concentration the liquid hourly space velocity decreased, which consequently
6
7 decreased the glycerol conversion and 1,2-PDO selectivity [65]. Mota et al. 2018 [70] have reported
8
9 that hydrogen in excess was the pre-requirement for acetol hydrogenation. This study suggested
10
11 that the maximum selectivity to 1,2-PDO was obtained in presence of the H₂/glycerol mole
12
13 ration of 66.8.
14
15

16
17
18 Reaction parameter study demonstrated that almost complete conversion of glycerol can
19
20 be achieved with the maximum 1,2-PDO selectivity to ~89 % at the optimum reaction condition
21
22 i.e. 220°C, 0.72 MPa, and at the WHSV of 0.07 h⁻¹. Based on the product distribution obtained in
23
24 presence of Cu-Zn/MgO catalyst, a probable two-steps reaction mechanism (Scheme 1) of
25
26 glycerol dehydration and hydrogenation can be proposed [38]. At temperature 190°C and 0.1 MPa
27
28 pressure acetol was detected as major product due to dehydration of glycerol. As shown in
29
30 Figure 5, the selectivity to acetol decreased continuously with simultaneous increase in 1,2-PDO
31
32 selectivity with the rise of temperature, pressure and catalyst weight, respectively. This results
33
34 indicated that, acetol was hydrogenated to 1,2-PDO at elevated reaction condition. Moreover, the
35
36 selectivity to ethylene glycol, methanol and ethanol were also increased at higher temperature
37
38 and pressure, which indicated that these degradation products were generated due to the C-C
39
40 bond cleavage of glycerol. 1-PO and 2-PO were the over hydrogenolysis product of 1,2-PDO, as
41
42 their selectivity were also increased at severe reaction condition.
43
44
45
46
47
48
49
50
51
52
53
54
55
56
57
58
59
60



Scheme 1. Reaction mechanism over Cu-Zn/MgO catalyst

Further, the stability of Cu-Zn/MgO catalyst was established by performing the time-on-stream study for 84 h at the optimum reaction condition obtained. Finally, the spent catalyst was characterized by XRD and TEM, and the structural properties of the fresh and used catalyst were compared which is discussed in the following section.

4.3.6. Time-on-stream stability

The stability of Cu-Zn/MgO catalyst was examined by performing the time-on-stream experiment and the results obtained are illustrated in Figure 6. The experiment was conducted at the optimum reaction condition as obtained from the parameter study. As shown in Figure 7, the glycerol conversion was almost 100% up to 75 h, further, it was slightly decreased. The selectivity to 1,2-PDO was ~89% up to 35 h and further, it was decreased ~5% with a simultaneous increase in selectivity to acetol. The activity and 1,2-PDO selectivity were reduced after a longer period of use might be due to increasing the degree of reduction of the catalyst as well as the agglomeration of active metal species present on the catalyst surface. Another

possible reason may be the reduction of active metal surfaces due to the adsorption of reactants and products during the time-on-stream study. The selectivity to other products was <5% throughout the reaction time. This result demonstrated that the Cu-Zn/MgO catalyst was very stable and selective for a longer period of time because ZnO helped to stabilize the copper species in the catalyst which were the pivotal sites for hydrogenolysis reaction [35, 36, 71].

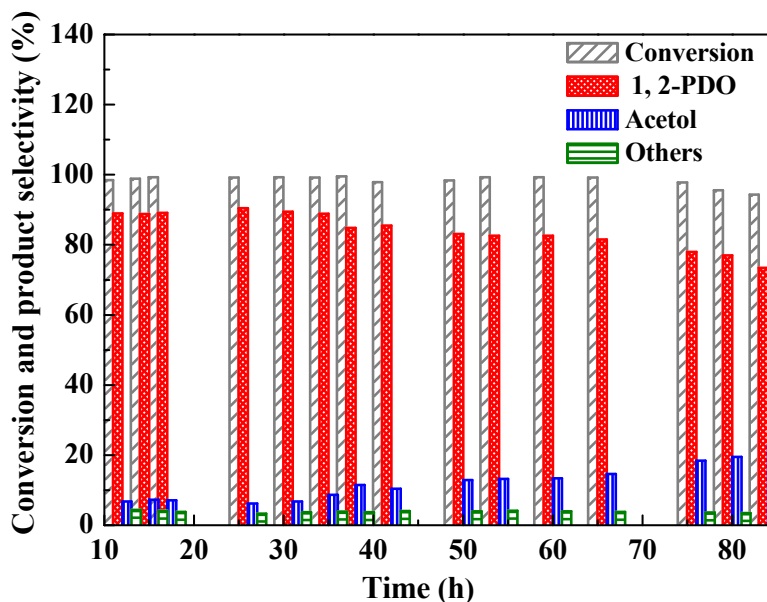


Figure 6. Time-on-stream study over Cu-Zn/MgO catalyst

Reaction condition: 220°C, 0.72 MPa, 10 wt.% aqueous glycerol as feed, catalyst 2.5 g, WHSV = 0.073 h⁻¹, H₂/glycerol mole ratio = 66.8.

4.4. Characterization of used catalyst

The structural properties of the spent Cu-Zn/MgO catalysts after 84 h of the reaction was characterized by performing XRD and TEM and the results were compared with the fresh catalyst characterization data (Figure 7). As shown in Figure 7 (A), the diffraction peaks corresponding to metallic copper was intact in the catalyst even after the uses of catalyst for a longer period of time. Moreover, it is very interesting to note that the intensity of the peaks

1
2
3 corresponding to metallic copper was increased significantly. This results suggested that, after
4
5 prolonging use of the catalyst in the hydrogen environment, the degree of reduction of copper
6
7 metal in the catalyst was increased significantly.
8
9
10

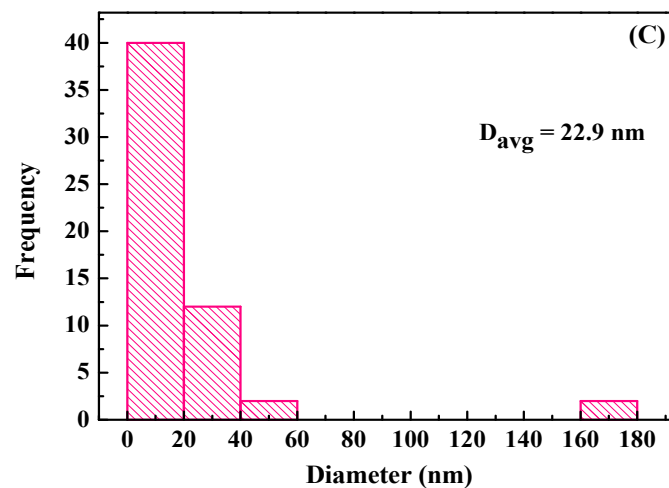
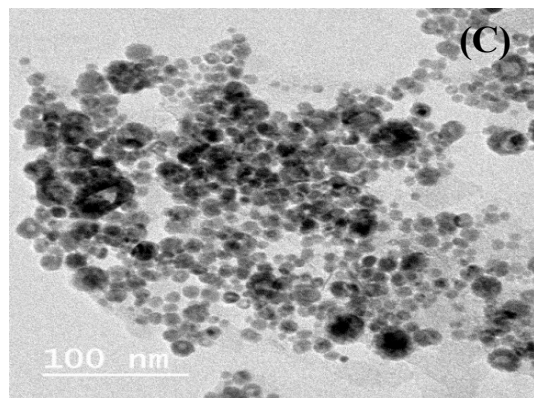
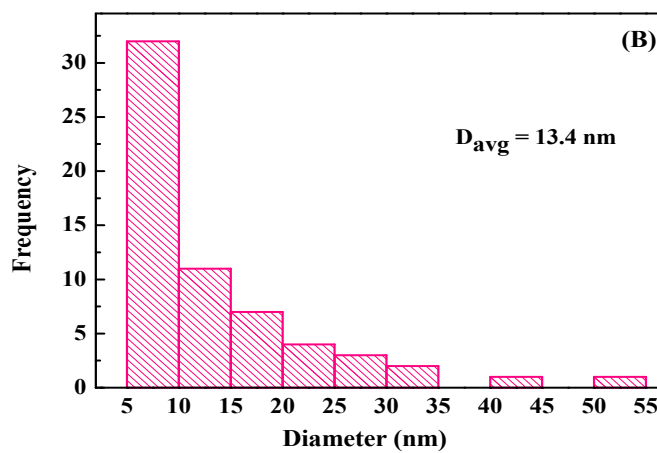
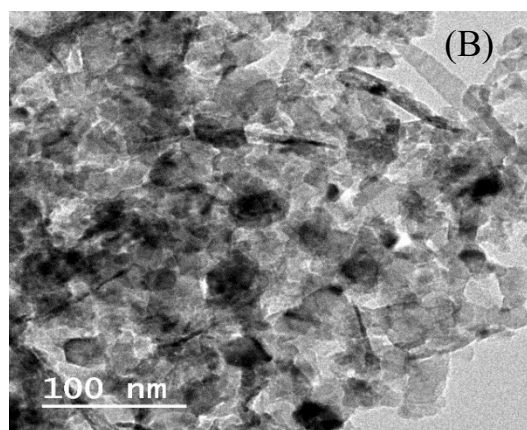
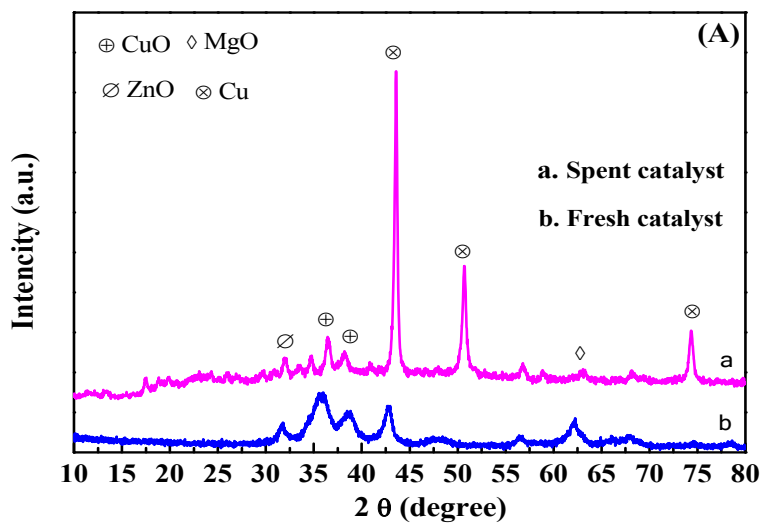


Figure 7. XRD pattern of fresh and spent catalyst (A), TEM image of fresh (B) and spent (C) catalyst

1
2
3 These results are also consistent with the TEM image of the used catalyst (Figure 7 (C)), where it
4 is clearly visible that the particle size in the used catalyst was more uniform as compared to the
5 fresh catalyst (Figure 7 (B)). The average metal particle size was calculated for fresh and spent
6 catalyst based on TEM analysis and it was found that the average metal particle size was slightly
7 increased from 13.4 nm to 22.9 nm in the spent catalyst may be due to particle agglomeration.
8
9

5. Conclusions

10
11
12 Catalytic performance of copper-zinc bimetallic catalysts over various support were
13 evaluated and compared for vapor phase hydrogenolysis of glycerol. catalysts characterization
14 results demonstrated a clear variation of metal support interaction with the variation of supports
15 for all the copper-zinc bimetallic catalysts. For all the catalysts, the average crystallite size of
16 copper metal particles was very small (<35 nm). Maximum copper metal dispersion of ~5% with
17 an active metal surface area of ~23 m². g⁻¹ was obtained for Cu-Zn/MgO catalyst. The TPD
18 results showed that Cu-Zn/MgO was most acidic in nature and the basicity was highest for Cu-
19 Zn/TiO₂ catalyst.
20
21
22
23
24
25
26
27
28
29
30
31
32
33
34
35
36
37
38
39
40

41 The catalytic activity results demonstrated that at atmospheric pressure CaO and MgO
42 supported catalyst were most active and acetol was obtained as a primary reaction product. At
43 atmospheric pressure, acetol was formed due to lower hydrogenation rate at low hydrogen
44 adsorption. MgO supported copper-zinc catalyst was found to be most selective to 1,2-PDO. The
45 higher selectivity to 1,2-PDO was attributed to higher basicity, very high metal dispersion
46 (~5%), highest copper metallic surface area (~23 m². g⁻¹). The product selectivity trend obtained
47 suggested two steps hydrogenolysis of glycerol i.e. dehydration to acetol followed by the
48
49
50
51
52
53
54
55
56
57
58
59
60

hydrogenation of acetol to 1,2-PDO. Reaction parameter study suggested lower temperature (<240°C), high pressure (>0.72 MPa) and low WHSV (< 0.07 h⁻¹) was favorable for higher selectivity to 1,2-PDO. Almost complete conversion (>98%) of glycerol with very high selectivity (89%) to 1,2-PDO was obtained in presence of Cu-Zn/MgO catalyst at 220°C, 0.72 MPa pressure and at the WHSV of 0.07 h⁻¹. The presence of Cu⁺⁺ and Cu⁺ on the MgO supported catalyst propagated the dehydration of glycerol to acetol and Cu⁰ activated the hydrogen molecule for hydrogenation of acetol to 1,2-PDO. Further, the time-on-stream study established the stability of the catalyst for a longer period of time with almost constant selectivity to 1,2-PDO. The catalytic stability also established by the characterization results of the used catalyst. Therefore, the Cu-Zn/MgO catalysts developed in this study may be a promising catalyst for the continuous production of 1,2-PDO by the hydrogenolysis of biodiesel derived glycerol on an industrial scale.

Conflict of interest

There is no conflict of interest

Acknowledgment

Authors thank Indian Institute of Technology Roorkee, Uttarakhand, India for providing facility to carry out the work. Authors also thanks Ministry of human resource and development (MHRD), Government of India, for the award of fellowship to carry out the work at IIT Roorkee.

References

1. M. Ayoub, A.Z. Abdullah, *Renew. Sustain. Energy Rev.*, 2012, 16, 2671–2686.
doi:10.1016/j.rser.2012.01.054

- 1
2
3 [2] R.C. Yang, F X; Hanna, M A; Sun, *Biotechnol. Biofuels.*, 2012, 5, 1–10.
4
5 doi.org/10.1186/1754-6834-5-13
6
7
8
9 [3] S. Bagheri, N.M. Julkapli, W.A. Yehye, *Renew. Sustain. Energy Rev.* 2015, 41, 113–127.
10 doi:10.1016/j.rser.2014.08.031.
11
12
13
14 [4] C.A.G. Quispe, C.J.R. Coronado, J.A. Carvalho, *Renew. Sustain. Energy Rev.*, 2013, 27,
15 475–493. doi:10.1016/j.rser.2013.06.017
16
17
18
19 [5] Y. Wang, J. Zhou, X. Guo, *RSC Adv.* 2015, 5, 74611–74628. doi:10.1039/c5ra11957j
20
21
22
23 [6] Y. Nakagawa, K. Tomishige, *Catal. Sci. Technol.*, 2011, 1, 179–190.
24 doi:10.1039/c0cy00054j
25
26
27
28 [7] A. Brandner, K. Lehnert, A. Bienholz, M. Lucas, P. Claus, *Top. Catal.*, 2009, 52, 278–
29 287. doi:10.1007/s11244-008-9164-2
30
31
32
33 [8] A. Marinas, P. Bruijninx, J. Ftouni, F.J. Urbano, C. Pinel, *Catal. Today.*, 2015, 239, 31–
34 37. doi:10.1016/j.cattod.2014.02.048
35
36
37
38
39 [9] Y. Nakagawa, M. Tamura, K. Tomishige, *J. Mater. Chem. A.*, 2014, 2, 6688–6702.
40 doi:10.1039/c3ta15384c
41
42
43
44 [10] S. Wang, K. Yin, Y. Zhang, H. Liu, *ACS Catal.*, 2013, 3, 2112–2121.
45 doi:10.1021/cs400486z
46
47
48
49
50 [11] R. Mane, S. Patil, M. Shirai, S. Rayalu, C. Rode, *Appl. Catal. B*, 2017, 204, 134–146.
51 doi:10.1016/j.apcatb.2016.11.032
52
53
54
55 [12] C.T.Q. Mai, F.T.T. Ng, *Catal. Today.*, 2017, 291, 195–203.
56
57
58
59
60

doi:10.1016/j.cattod.2017.02.043

- [13] E. Gallegos-Suarez, A. Guerrero-Ruiz, I. Rodriguez-Ramos, A. Arcoya, Chem. Eng. J., 2015, 262, 326–333. doi:10.1016/j.cej.2014.09.121
- [14] S.K. Tanielyan, N. Marin, G. Alvez, R. Bhagat, B. Miryala, R.L. Augustine, S.R. Schmidt, Org. Process Res. Dev., 2014, 18, 1419–1426. doi:10.1021/op400123f
- [15] H. Tan, M.N. Hedhill, Y. Wang, J. Zhang, K. Li, S. Sioud, Z.A. Al-Talla, M.H. Amad, T. Zhan, O.E. Tall, Y. Han, Catal. Sci. Technol., 2013, 3, 3360. doi:10.1039/c3cy00661a
- [16] J. Zheng, W. Zhu, C. Ma, Y. Hou, W. Zhang, Z. Wang, React. Kinet. Mech. Catal., 2010, 99, 455–462. doi:10.1007/s11144-009-0127-9
- [17] S.M. Pudi, P. Biswas, S. Kumar, B. Sarkar, J. Braz. Chem. Soc., 2015, 26, 1551–1564. doi:10.5935/0103-5053.20150123
- [18] H. Zhao, L. Zheng, X. Li, P. Chen, Z. Hou Catalysis Today xxx (xxxx) xxx–xxx.
<https://doi.org/10.1016/j.cattod.2019.03.011>
- [19] E.S. Vasiliadou, A.A. Lemonidou, Appl. Catal. A Gen., 2010, 396, 177–185. doi:10.1016/j.apcata.2011.02.014
- [20] A. Perosa, P. Tundo, Ind. Eng. Chem. Res., 2005, 44, 8527–8535. doi:10.1021/ie0489251
- [21] S. Sato, M. Akiyama, R. Takahashi, T. Hara, K. Inui, M. Yokota, Appl. Catal. A Gen., 2008, 347, 186–191. doi:10.1016/j.apcata.2008.06.013
- [22] M. Akiyama, S. Sato, R. Takahashi, K. Inui, M. Yokota, Appl. Catal. A Gen., 2009, 371, 60–66. doi:10.1016/j.apcata.2009.09.029

- 1
2
3 [23] A. Bienholz, H. Hofmann, P. Claus, *Appl. Catal. A Gen.* 2011, 391, 153–157.
4
5 doi:10.1016/j.apcata.2010.08.047
6
7
8 [24] D. Sun, Y. Yamada, S. Sato, *Appl. Catal. A Gen.*, 2014, 475, 63–68.
9
10 doi:10.1016/j.apcata.2014.01.015
11
12
13 [25] V. Pavan kumar, C.S. Srikanth, A.N. Rao, K.V.R. Chary, *J. Nanosci. Nanotechnol.*, 2014,
14
15 14, 3137–3146. doi:10.1166/jnn.2014.8544
16
17
18 [26] L. Huang, Y. Zhu, H. Zheng, G. Ding, Y. Li, *Catal. Letters.* 2009, 131, 312–320.
19
20 doi:10.1007/s10562-009-9914-1
21
22
23 [27] R.B. Mane, A.A. Ghalwadkar, A.M. Hengne, Y.R. Suryawanshi, C. V. Rode, *Catal.*
24
25 *Today.* 2011, 164, 447–450. doi:10.1016/j.cattod.2010.10.032
26
27
28 [28] D. Sun, Y. Yamada, S. Sato, *Appl. Catal. B*, 2015, 174–175, 13–20.
29
30 doi:10.1016/j.apcatb.2015.02.022
31
32
33 [29] N.N. Pandhare, S.M. Pudi, P. Biswas, S. Sinha, *J. Taiwan Inst. Chem. Eng.*, 2016, 61, 90–
34
35 96. doi:10.1016/j.jtice.2015.12.028
36
37
38
39
40
41 [30] N.N. Pandhare, S.M. Pudi, P. Biswas, S. Sinha, *Org. Process Res. Dev.*, 2016, 20, 1059–
42
43 1067. doi:10.1021/acs.oprd.6b00110
44
45
46
47 [31] S. Sato, M. Akiyama, K. Inui, M. Yokota, *Chem. Lett.*, 2009, 38, 560–561.
48
49 doi:10.1246/cl.2009.560
50
51
52 [32] L. Huang, Y.-L. Zhu, H.-Y. Zheng, Y.-W. Li, Z.-Y. Zeng, *J. Chem. Technol. Biotechnol.*,
53
54 2008, 83, 1670–1675. doi:10.1002/jctb.1982
55
56
57
58
59
60

- 1
2
3 [33] M. Harisekhar, V. Pavan Kumar, S. Shanthi Priya, K.V.R. Chary, J. Chem. Technol.
4 Biotechnol., 2015, 90, 1906–1917. doi:10.1002/jctb.4728
5
6
7
8
9 [34] M. Lee, Y.K. Hwang, J.S. Chang, H.J. Chae, D.W. Hwang, Catal. Commun., 2016, 84, 5–
10 10. doi:10.1016/j.catcom.2016.05.022
11
12
13
14 [35] R.P. Ye, L. Lin, Q. Li, Z. Zhou, T. Wang, C.K. Russell, H. Adidharma, Z. Xu, Y.G. Yao,
15 M. Fan, Catal. Sci. Technol., 2018, 8, 3428–3449. doi:10.1039/c8cy00608c done
16
17
18
19 [36] L. Zheng, X. Lia, W. Du, D. Shi, W. Ning, X. Lu, Z. Hou, App Catal B, 2017, 203, 146–
20 153. oi.org/10.1016/j.apcatb.2016.10.011
21
22
23 [37] S. Xia, R. Nie , X. Lu , L. Wang, P. Chen, Z Hou, J. Catal 296 (2012) 1–11
24
25
26 [38] M.A. Dasari, P.P. Kiatsimkul, W.R. Sutterlin, G.J. Suppes, Appl. Catal. A Gen., 2005,
27 281, 225–231. doi:10.1016/j.apcata.2004.11.033 +2
28
29
30 [39] C. Montassier, J.C. Menezo, L.C. Hoang, C. Renaud, J. Barbier, J. Mol. Catal.,1991, 70
31 99–110. doi:10.1016/0304-5102(91)85008-P
32
33
34
35 [40] E.P. Maris, W.C. Ketchie, M. Murayama, R.J. Davis, J. Catal., 2007, 251, 281–294.
36 doi:10.1016/j.jcat.2007.08.007
37
38
39
40
41 [41] Z. Wu, Y. Mao, M Song, X. Yin, M. Zhang. Catal. Comm, 2013, 32,52– 57.
42
43 [42] L. Guo, J. Zhou, J. Mao, X. Guo, S. Zhang. App Cata A: Gen., 2009,367, 93–98.
44
45 [43] A. Marinoiu G. Ionita, C.L. Gaspar, C. Cobzaru, S. Oprea React Kinet Catal Lett. 2009,
46 97, 315–320.
47
48
49
50 [44] M. Balaraju, V. Rekha, P.S.S. Prasad, R.B.N Prasad, N. Lingaiah, Catal Lett, 2008 126,
51 119-124. doi: 10.1007/s10562-008-9590-6
52
53
54
55
56
57
58
59
60

- 1
2
3 [45] M.L. Shoji, V. D. B. C. Dasireddy, S. Singh, P. Mohlala, D. J. Morgan, H. B. Friedrich,
4 ACS Sustainable Chem. Eng. 2016, 4, 5752–5760. DOI:0.1021/acssuschemeng.6b01675
5
6
7 [46] L. Niu, R. Wei, H. Yang, X. Li, F. Jiang, G. Xiao. Chin. J. Catal 2013, 34, 2230–2235.
8
9
10 [47] S. Xia, Z. Yuan, L. Wang, P. Chen, Z. Hou Appli. Catal A: Gen., 2011, 403, 173– 182.
11 doi:10.1016/j.apcata.2011.06.026
12
13 [48] Y.T. Kim, K.-D. Jung, E.D. Park, Appl. Catal. B, 2011, 107, 177–187.
14
15
16 [49] M. Massa, A. Andersson, E. Finocchio, G. Busca J. Catal, 2013, 307,170–184.
17 http://dx.doi.org/10.1016/j.jcat.2013.07.022
18
19
20 [50] Z. Wang, L. Wang, Y. Jiang, M. Hunger, J. Huang, ACS Catal., 2014, 4, 1144–1147.
21 dx.doi.org/10.1021/cs401225k
22
23
24 [51] V. Montes, M. Checa, A. Marinas, M. Boutonnet, J.M. Marinas, F.J. Urbano, S. J. Pinel
25 Catal. Today, 2014, 223, 129– 137. http://dx.doi.org/10.1016/j.cattod.2013.09.021
26
27
28 [52] C. Xu, Y. Du, C. Li, J. Yang, G. Yang, Appl. Catal. B, 2015, 164 334–343.
29 doi:10.1016/J.APCATB.2014.09.048
30
31
32 [53] M. Kruk, M. Jaroniec, Chem. Mater. 2001, 13, 3169–3183. doi:10.1021/CM0101069
33
34
35
36 [54] V. Rekha, C. Sumana, S.P. Douglas, N. Lingaiah, Appl. Catal. A Gen., 2015, 491, 156–
37 162. doi:10.1016/j.apcata.2014.10.042
38
39
40
41 [55] S. Wang, H. Liu, Catal. Letters. 117 (2007) 62–67. doi:10.1007/s10562-007-9106-9
42
43
44
45 [56] A. Al Ameen, S. Mondal, S.M. Pudi, N.N. Pandhare, P. Biswas, Energy Fuels, 2017, 31,
46 8521–8533. doi:10.1021/acs.energyfuels.7b00766
47
48
49
50 [57] N.D. Kim, S. Oh, J.B. Joo, K.S. Jung, J. Yi, Korean J. Chem. Eng., 2010, 27, 431–434.
51 doi:10.1007/s11814-010-0070-5
52
53
54
55
56
57
58
59
60

- 1
2
3 [58] Z. Huang, F. Cui, H. Kang, J. Chen, *Chem. Mater.*, 2008 5090–5099. doi:doi:
4 10.1021/cm8006233
5
6
7
8
9 [59] T. Miyazawa, Y. Kusunoki, K. Kunimori, K. Tomishige, *J. Catal.*, 2006, 240, 213–221.
10 doi:10.1016/j.jcat.2006.03.023
11
12
13
14 [60] E. D’Hondt, S. V. D. Vyver, B.F. Sels, P.A. Jacobs, *Chem. Commun.*, 2008, 6011–6012.
15 doi:10.1039/b812886c
16
17
18
19 [61] S. Panyad, S. Jongpatiwut, T. Sreethawong, T. Rirksomboon, S. Osuwan, *Catal. Today*,
20 2011, 174, 59–64. doi:10.1016/j.cattod.2011.03.029
21
22
23
24 [62] F. Vila, M. Lopez Granados, M. Ojeda, J.L.G. Fierro, R. Mariscal, *Catal. Today*, 2012,
25 187, 122–128. doi:10.1016/j.cattod.2011.10.037
26
27
28
29 [63] Z. Xiao, X. Wang, J. Xiu, Y. Wang, C.T. Williams, C. Liang, *Catal. Today*, 2014, 234,
30 200–207. doi:10.1016/j.cattod.2014.02.025
31
32
33
34 [64] Q. Gao, B. Xu, Q. Tong, Y. Fan, *Biosci. Biotechnol. Biochem.*, 2016, 80, 215–220.
35 doi:10.1080/09168451.2015.1088372
36
37
38
39
40
41 [65] H. Mitta, P.K. Seelam, S. Ojala, R.L. Keiski, P. Balla, *Appl. Catal. A Gen.*, 2018, 550,
42 308–319. doi:10.1016/j.apcata.2017.10.019
43
44
45
46 [66] P.K. Vanama, A. Kumar, S.R. Ginjupalli, V.R.C. Komandur, *Catal. Today*, 2015, 250,
47 226–238. doi:10.1016/j.cattod.2014.03.036
48
49
50
51 [67] S. Mondal, A.A. Arifa, P. Biswas, *Catalyst, Catal. Letters.*, 2017, 147, 2783–2798.
52 doi:10.1007/s10562-017-2187-1
53
54
55
56
57
58
59
60

- 1
2
3 [68] R.B. Mane, A.M. Hengne, A.A. Ghalwadkar, S. Vijayanand, P.H. Mohite, H.S. Potdar, C.
4 V. Rode, *Catal. Letters.*, 2010, 135, 141–147. doi:10.1007/s10562-010-0276-5
5
6
7
8
9 [69] M.L. Dieuzeide, R. de Urriaga, M. Jobbagy, N. Amadeo, *Catal. Today*, 2017, 296, 19–25.
10 doi:10.1016/j.cattod.2017.05.095
11
12
13
14 [70] C.J.A. Mota, V.L.C. Gonçalves, J.E. Mellizo, A.M. Rocco, J.C. Fadigas, R. Gambetta, J.
15 Mol. Catal. A Chem., 2016, 422, 158–164. doi:10.1016/j.molcata.2015.11.014
16
17
18
19 [71] T. Jiang, D. Kong, K. Xu, F. Cao, *Appl. Petrochemical Res.*, 2015, 5 221–229.
20 doi:10.1007/s13203-015-0125-y
21
22
23
24 [72] Z. Yuan, W. Lina, J. Wang, S. Xiaa, P. Chen, Z. Hou, X. Zheng *Appl Catal B: Environ*,
25 2011, 101, 431–440.
26
27
28
29 [73] L. Zheng, S. Xia, Z. Hou, *Appl. Clay Sci.* 2015, 118, 68–73.
30 http://dx.doi.org/10.1016/j.clay.2015.09.002
31
32
33
34 [74] Y. Feng, H. Yin, A. Wang, L. Shen, L.Yu, T. Jiang, *Chem Eng J.* 2011, 168, 403–412.
35
36
37 [75] E.S Vasiliadou, A.A. Lemonidou *App Catal A: General* 396 (2011) 177–185
38 doi:10.1016/j.apcata.2011.02.014
39
40
41 [76] C.W. Chiu, A. Tekeei, W.R. Sutterlin, J. M. Ronco, G. J. Suppes *AIChE Journal* 2008
42 54(9) 2456-2463
43
44
45 [77] S. Mondal, H. Malviya. P. Biswas *React. Chem. Eng.*, 2019, 4, 595-609
46 Doi: 10.1039/C8RE00138C
47
48
49
50 [78] X. Lin, Y. Lv, Y. Xi, Y. Qu, D. L. Phillips, C. Liu *Energy Fuels* 2014, 28, 3345–3351
51 dx.doi.org/10.1021/ef500147k
52
53
54
55
56
57
58
59
60

Research highlight

- Highly promising Cu-Zn/MgO catalyst was synthesized for the production of propylene glycol (1,2-propanediol) by the vapor phase hydrogenolysis of glycerol.
- Very high glycerol conversion of 98.5% with ~89% selectivity to propylene glycol was achieved at very low pressure (0.72 MPa).
- Uniform distribution of metal particles, the presence of partially reduced copper species (Cu_2O , CuO , Cu^0) and higher basicity were the governing factor for higher selectivity to propylene glycol.
- The catalyst was found to be highly durable and selective to propylene glycol.

Graphical abstract

